

HYDRODYNAMIC ANALYSIS OF A FIXED INCLINE SLIDER BEARING

J. K. Limo¹, J. K. Bitok², A. W. MANYONGE³ AND C. C. WANJALA⁴

¹ Department of Mathematics and Computer Science
Laikipia University, P.O. BOX 1100-20300 Nyahururu, Kenya
E-mail: limojoshua@yahoo.com

² Department of Mathematics and Computer Science
University of Eldoret, P.O. BOX 1125-30100 Eldoret, Kenya
E-mail: jacobbitok@yahoo.com

^{3,4} Department of Pure and Applied Mathematics,
Maseno University, Private Bag, 40105, Maseno, Kenya
E-mail: ³ amanyonge@maseno.ac.ke, ⁴ iyaya_wanjala@yahoo.com

Abstract

In the present day technological scenario, machines rotating at high speeds and carrying heavy rotor loads are used. As a result, fixed incline slider bearings are used. They are designed for high axial loads. When a bearing rotates at high speed, the heat generated due to large shearing rates in the lubricant film raises its temperature which lowers the viscosity of the lubricant and in turn affects the performance characteristics of the bearing. Hydrodynamic analysis should therefore be done to obtain the realistic performance characteristics of the bearing. In most of the analyses, two dimensional energy Equation is used to find the temperature distribution in the fluid film by neglecting the temperature variation in the axial direction. In this research, two dimensional study will be done to predict pressure and the temperature distribution along a fixed incline slider bearing surface axially. The numerical results obtained for the pressure profiles, temperature profiles,

Key Words and Phrases : *Reynolds Equation, Axial load, Pressure, Fixed inclined slider bearing.*

2000 AMS Subject Classification : 82D80.

© <http://www.ascent-journals.com>

velocity profiles, will be analyzed, discussed and represented graphically. The friction coefficient and power loss of the bearing will also be determined, analyzed and represented graphically. The results obtained here will be useful in designing and modifying fluid dynamic bearings.

1. Introduction

Machines consist of elements and their safe and efficient operation relies on carefully designed interfaces between these elements. The functional design of interfaces cover geometry; materials, lubrication and surface topography, and an incorrect design may lead to both lowered efficiency and shortened service life. A misalignment due to geometrical design could lead to large stress concentrations that in turn may lead to severe damage when mounting, a detrimental wear situation and rapid fatigue during operation. Large stress concentrations also implicitly imply a temperature rise because of the energy dissipation due to plastic deformations. This means that the choice of mating materials is also of great importance such as, electrolytic corrosion may drastically reduce service life. Contact fatigue due to low ductility would not only lower the service life but could lead to third body abrasion due to spalling, which in turn could end up lowering the service life of other components. A lubricant serves several crucial objectives; with its main objective being to lower friction, the actions of additives are of concern. If the interface is subjected to excessive wear, the lubricants ability to form a separating film becomes even more crucial. In this case, the bulk properties of the lubricant have to be carefully chosen. At some scale, regardless of the surface finish, all real surfaces are rough and their topography influences the contact condition. As implied above, these design parameters are mutually dependent i.e. they affect the way lubricants properties and geometry influence the operation of the system. For example, a change in geometry could require another choice of materials that may change the objectives of the lubricant and force the operation into another lubrication regime. All the four design parameters are of great importance. However, in our research, focus will be on the lubricant properties such as pressure, temperature, viscosity and the geometry of the bearing and how it affects the performance characteristics of the bearing. A number of models of hydrodynamic bearings have been proposed over the years. Vohr [1] described an analytical method for predicting the operating temperature of thrust bearings of the size and speed found in large vertical machines. He predicted bearing

operating temperatures showing excellent agreement with laboratory tests and with field measurements over a wide range of bearing sizes and operating conditions. Abdel-Latif [2] investigated the centrifugal effects of thermo-hydrodynamic performance of circular pad thrust bearings. He showed that the upper limits of laminar operation, centrifugal forces alter considerably the load, the frictional force and the lubricant inflow and can either over estimate or underestimate the bearing performance characteristics, depending on the pads geometry and the operating conditions of the bearing. Hashimoto [3] analyzed the performance characteristics of sector-shaped pad thrust bearing in turbulent inertial flow regime under three types of lubrication conditions. He solved the momentum equation in terms of pressure and stream function by applying numerical calculation technique combining control volume, integration and the Newton-Raphson linearization method under three kinds of inlet boundaries in relation to the three types of lubrication conditions namely; the flooded condition, the over flooded condition and the starved condition. Fenner [4] studied a three-dimensional thermo-hydrodynamic analysis of pivoted pad thrust bearings. He described a method for predicting the performance of pivoted pad thrust bearings. He then compared the theoretical results he obtained with experimental results. Kiogora et. al. [5] developed a conservative scheme model of an inclined pad thrust bearing. They also obtained a numerical solution of the momentum and energy equations of an inclined pad thrust bearing. Banwait et. al. [6] studied thermo-hydrodynamic analysis to investigate the influence of modified viscosity-temperature equation on a plain journal bearing. They used finite difference method to predict temperature distribution in a journal bearing. They found the temperature distribution along the axial direction of the journal using a steady state unidirectional heat conduction equation. Charitupoulous et. al. [7] did a computational investigation of thermo-hydrodynamic performance and mechanical deformations of fixed geometry thrust bearing with artificial surface texturing. Although a lot of research has been done in the last two decades, hydrodynamic analysis of an fixed incline slider bearing to determine its performance by considering axial variation of pressure, viscosity and temperature, load and the geometry of the bearing has not been researched on extensively and this is what this research strives to explore.

2. Assumptions and Approximations

In the mathematical analysis, the lubricant to be used in a fixed incline slider bearing, the following assumptions will be made;

- i. Inertia and body force terms are negligible as compared to viscous and pressure forces
- ii. The lubricant is incompressible
- iii. There is no variation of pressure across the fluid film
- iv. There is no slip in the fluid solid boundary
- v. No external forces act on the film.

3. Mathematical Model

Consider the flow of a Newtonian viscous incompressible fluid(lubricant) of constant density and coefficient of viscosity with velocity vector \mathbf{q} having velocity components u , v , w in the x -, y - and z - directions respectively and pressure p . The basic governing equations of fluid dynamics based on the assumptions above are;

3.1 Conservation of Mass Equation

In three dimensions, the equation of continuity as given for example by Manyonge [8] is;

$$\frac{\partial \rho}{\partial t} + \frac{(\partial \rho u)}{\partial x} + \frac{(\partial \rho v)}{\partial y} + \frac{(\partial \rho w)}{\partial z} = 0 \quad (1)$$

If the density is constant, then $(\partial \rho)/(\partial t) = 0$, and the above equation reduces to;

$$\frac{\partial u}{\partial x} + \frac{\partial v}{\partial y} + \frac{\partial w}{\partial z} = 0 \quad (2)$$

which is the equation of continuity for an incompressible fluid.

3.2 Conservation of Momentum Equation

This is derived from Newton's second law of motion which states that the sum of resultant forces is equal to rate of change of momentum of the flow. The momentum equation in is written as;

$$\frac{\partial \mathbf{q}}{\partial t} + (\mathbf{q} \cdot \nabla) \mathbf{q} = -\frac{1}{\rho} \nabla p + \frac{1}{\rho} \nabla \cdot \boldsymbol{\tau} + \mathbf{F} \quad (3)$$

where τ is the viscous shear stress. The Reynolds equation for a fixed inclined slider bearing as given by Sahu [9] is ;

$$\frac{\partial}{\partial x}(h^3 \frac{\partial p}{\partial x}) + \frac{\partial}{\partial y}(h^3 \frac{\partial p}{\partial y}) = 12u\eta_0 \frac{\partial h}{\partial x} \quad (4)$$

with parameters as defined in the nomenclature.

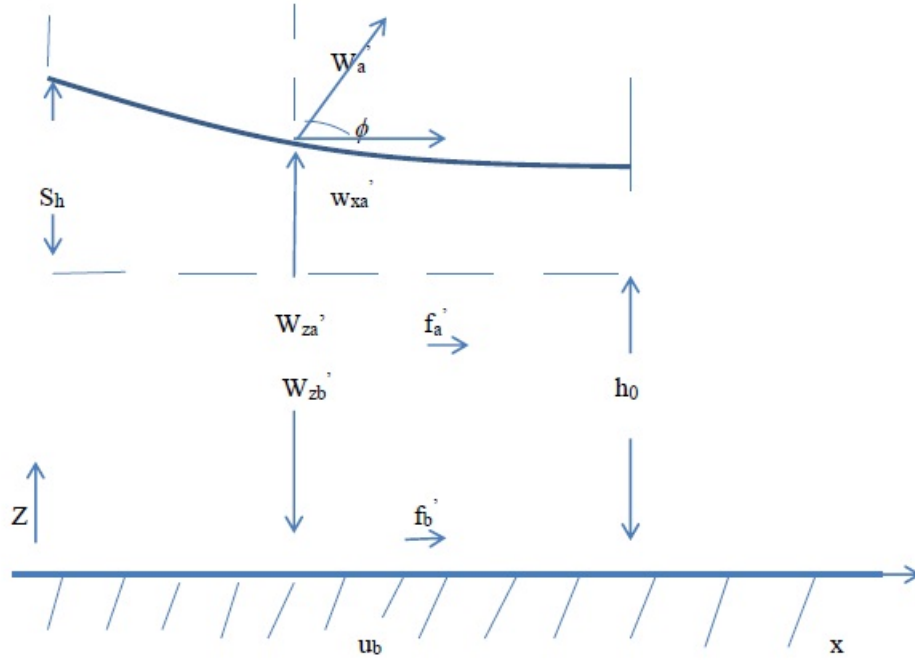


Figure 1: Force components and oil film geometry in a hydro dynamically lubricated thrust sector.

4. Theoretical Analysis

4.1 Force Components and Oil Film Geometry

The forces acting on the solids can be considered in two groups. The loads, which act in the direction normal to the surface, yield normal loads that can be resolved into components w'_x and w'_z . The viscous surface stresses, which act in the direction tangent to the surface, yield shear forces on the solids that have components f' in the x - direction. The component of the shear forces in the z - direction is negligible. Once

the pressure is obtained for a particular film configuration from the Reynolds equation, the following force components act on the solids:

$$w'_{za} = w'_{zb} = \int_0^l p dx \quad (5)$$

$$w'_{zb} = 0 \quad (6)$$

$$w'_{xa} = - \int_{h_0+s_h}^{h_0} p dh = - \int_0^l \frac{dh}{dx} dx$$

Therefore

$$w'_{xa} = -(ph|_0^l) + \int_0^l h \frac{dp}{dx} dx = \int_0^l \frac{dp}{dx} dx \quad (7)$$

$$w'_b = \sqrt{((w'_{zb})^2 + (w'_{xb})^2)} = w'_{xb} \quad (8)$$

$$w'_a = \sqrt{((w'_{za})^2 + (w'_{xa})^2)} \quad (9)$$

$$\phi = \tan^{-1}\left(\frac{w'_{xa}}{w'_{za}}\right) \quad (10)$$

Shear forces per unit width acting on the solids are;

$$f'_b = \int_0^l (\tau_{zx})_{z=0} dx$$

But,

$$(\tau_{zx})_{z=0} = \left(\eta \frac{\partial u}{\partial z} \right)_{z=0} = -\frac{h}{2} \frac{\partial p}{\partial x} - \eta \frac{(u_b - u_a)}{h}$$

Therefore substituting this in the equation above gives;

$$f'_b = \int_0^l \left(\frac{-h}{2} \frac{dp}{dx} - \eta \frac{u_b}{h} \right) dx$$

Also;

$$f'_b = -\frac{w'_{xa}}{2} - \int_0^l \frac{\eta u_b}{h} dx \quad (11)$$

Similarly the shear force per unit width acting on the solid a is;

$$f'_a = - \int_0^l (\tau_{zx})_{z=h} dx = -\frac{w'_{xa}}{2} + \int_0^l \frac{\eta u_b}{h} dx \quad (12)$$

Note from figure (3) that;

$$f'_a + f'_b + w'_{xa} = 0 \quad (13)$$

$$w'_{zb} - w'_{xa} = 0 \quad (14)$$

These equations represent the condition of static equilibrium. The viscous stresses generated by the shearing of the lubricant film give rise to a resisting force of magnitude $-f_b$ on the moving surface. The rate of working against the viscous stresses, or power loss is

$$h_p = -f_b u_b = -f'_b (r_o - r_i) u_b \quad (15)$$

The work done against the viscous stresses appears as heat within the lubricant. Some of this heat may be transferred to the surroundings by radiation or by conduction, or it may be convected from the clearance space by the lubricant flow. The bulk temperature rise of the lubricant for the case in which all the heat is carried away by convection is known as the "adiabatic temperature rise." This bulk temperature increase can be calculated by equating the rate of heat generated within the lubricant to the rate of heat transferred by convection:

$$h_p = \rho q C_p (\Delta t_m)$$

Or the adiabatic temperature rise in degrees Celsius may be expressed as;

$$\Delta t_m = \frac{h_p}{\rho q C_p} \quad (16)$$

We are therefore going to use the equations above to analyze a fixed incline slider bearing. In our analysis, we will make use of non-dimensionlization to define the resulting performance parameters of the bearing. We will assume that the pressure generating mechanism is the physical wedge.

4.2 Fixed Incline Slider Bearing

The diagram of a fixed incline slider bearing is shown in figure 1a below. It is composed of a bottom plane surface that moves with uniform velocity u_b and a fixed inclined top surface. The region between them is full of lubricant. The oil film thickness is h at any point. The inlet clearance is $h_0 + s_h$. The outlet clearance is h_0 . The direction of motion and the inclination of planes are such that a converging oil film is formed between the surfaces and the physical wedge pressure-generating mechanism is developed in the oil film; it is this pressure-generating mechanism that makes the bearing able to support a load.

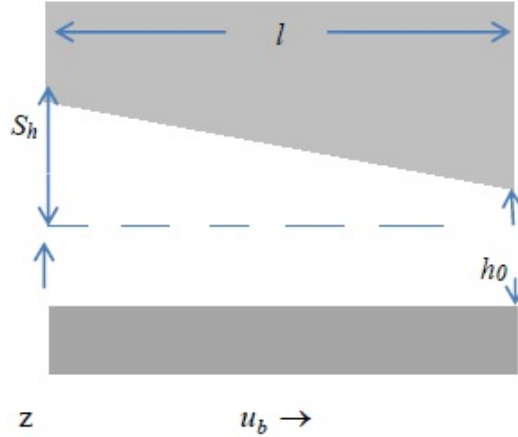


Figure 2 : Graph of dimensionless pressure, P versus X

4.3 Pressure Distribution

For hydro-dynamic lubrication, the Reynolds equation is given by;

$$\frac{\partial}{\partial x} \left(h^3 \frac{\partial p}{\partial x} \right) + \frac{\partial}{\partial y} \left(h^3 \frac{\partial p}{\partial y} \right) = 12u\eta \frac{\partial h}{\partial x} \quad (17)$$

Neglecting side leakages, equation (17) becomes;

$$\frac{\partial}{\partial x} \left(\rho h^3 \frac{\partial p}{\partial x} \right) = 12u\eta \frac{\partial(\rho h)}{\partial x} \quad (18)$$

Integrating this equation with respect to x gives;

$$\frac{1}{\eta} \frac{dp}{dx} = \frac{12u}{h^2} + \frac{A}{\rho h^3} \quad (19)$$

where A is a constant. Making use of the boundary conditions that; $dp/dx = 0$ when $x = x_m$, $\rho = \rho_m$ and $h = h_m$ gives; $A = -12u\rho_m h_m$. Substituting this into equation (19) gives;

$$\frac{dp}{dx} = 12u\eta \frac{\rho h - \rho_m h_m}{\rho h^3} \quad (20)$$

This is the integrated form of the Reynolds equation. The subscript m refers to the condition at all points where $dp/dx = 0$ such as the point of maximum pressure. If the density does not vary much throughout the conjunction, then it can be considered constant and equation (20) reduces to;

$$\frac{dp}{dx} = 12u\eta \frac{h - h_m}{h^3} \quad (21)$$

We will begin the analysis of a fixed incline slider bearing with the integrated form of Reynolds Equation (21) above. Keeping in mind that $u = (u_a + u_b)$. If we let $u_a = 0$, and assuming a constant viscosity η_0 , Equation (21) becomes;

$$\frac{dp}{dx} = 6u_b\eta_0 \frac{h - h_m}{h^3}$$

where h_m is the film thickness when $dp/dx = 0$. The oil film thickness can be written as a function of x i.e.

$$h = h_0 + s_h \left(1 - \frac{x}{l}\right) \quad (22)$$

Expressing the film thickness and pressure in dimensionless terms, we have;

$$P = \frac{ps_h^2}{\eta_0 u_b l}, \quad H = \frac{h}{s_h}, \quad H_m = \frac{h_m}{s_h}, \quad H_0 = \frac{h_0}{s_h} \quad \text{and} \quad X = \frac{X}{l} \quad (23)$$

Incorporating this in Equations (21) and (22) gives,

$$\frac{dP}{dX} = 6 \left(\frac{H - H_m}{H^3} \right) \quad (24)$$

$$H = \frac{h}{s_h} = H_0 + 1 - X \quad (25)$$

$$\frac{dH}{dX} = -1 \quad (26)$$

Integrating equation (24) gives;

$$P = 6 \int \left(\frac{1}{H^2} - \frac{H_m}{H^3} \right) dX \quad (27)$$

Making use of equation (26), we have;

$$P = 6 \int \left(\frac{1}{H^2} - \frac{H_m}{H^3} \right) dH$$

which when integrated gives

$$P = 6 \left(\frac{1}{H} - \frac{H_m}{2H^2} \right) + A \quad (28)$$

where A is a constant of integration. The boundary conditions are;

1. $P = 0$ when $X = 0 \Rightarrow H = H_0 + 1$
2. $P = 0$ when $X = 1 \Rightarrow H = H_0$

Making use of boundary conditions 1 and 2 we get;

$$H_m = \frac{2H_0(1 + H_0)}{1 + 2H_0} \quad \text{and} \quad A = -\frac{6}{1 + 2H_0} \quad (29)$$

Substituting equations (29) into (28) gives;

$$P = \frac{6X(1 - X)}{(H_0 + 1 - X)^2(1 + 2H_0)} \quad (30)$$

Next, we determine the maximum pressure for the fixed incline slider bearing, the pressure is maximum when, $dP/dX = 0$, $X = X_m$ and $H = H_m$. Therefore substituting this in (30), we obtain;

$$H_m = H_0 + 1 - X_m$$

Rearranging, We have;

$$X_m = \frac{1 + H_0}{1 + 2H_0} \quad (31)$$

Substituting this in equation (30), we have;

$$P_m = \frac{3}{2H_0(1 + H_0)(1 + 2H_0)} \quad (32)$$

In dimensionless terms, equation (32) becomes

$$P_m = \frac{3\eta_0 u_b l s_h}{2h_0(s_h + h_0)(s_h + 2h_0)} \quad (33)$$

4.4 Power Loss and Temperature Rise

The total rate of working against the viscous stresses, or the power loss, can be expressed from (15) as, $h_p = -f_b u_b = -f'_b(r_0 - r_i)u_b$. Expressed in dimensionless form,

$$H_p = \frac{h_p s_h}{\eta_0 u_b^2 l (r_0 - r_i)} = -\frac{f'_b s_h}{\eta_0 u_b l} = F_b$$

or

$$H_P = -4 \ln \left(\frac{H_0}{H_0 + 1} \right) - \frac{6}{1 + 2H_0} \quad (34)$$

All the heat produced by viscous shearing is assumed to be carried away by the lubricant(adiabatic condition) The bulk temperature increase can be calculated by equating the rate of heat generated within the lubricant to the rate of heat transferred by convection. Therefore from equation (16), the lubricant temperature rise is;

$$\Delta t_m = \frac{h_p}{\rho_0 q'_x C_p} = \frac{2u_b l \eta_0 H_p}{\rho_0 C_p s_h^2 Q} \quad (35)$$

where ρ_0 is the constant lubricant density, Kg/m^3 , q'_x is the volume flow rate per unit width in sliding direction, m^2/s and C_p is the specific heat capacity at constant pressure J/kgC . The dimensionless temperature rise may be expressed as;

$$\frac{H_p}{Q} = \frac{\rho_0 C_p s_h^2 \Delta t_m}{2u_b l \eta_0} = \frac{2(1 + 2H_0)}{H_0(1 + H_0)} \ln \left(\frac{H_0 + 1}{H_0} \right) - \frac{3}{H_0(1 + H_0)} \quad (36)$$

5. Results and Discussion

From equation (30) dimensionless pressure, P is a function of X and H_0 .

Table 1 : The variation of P with X for various values of H_0 ;

X	0	0.2	0.4	0.6	0.8	1.0
$H_0 = 2, P$	0	0.0245	0.0426	0.05	0.0397	0
$H_0 = 1, P$	0	0.0988	0.1875	0.2449	0.2222	0
$H_0 = 1/2, P$	0	0.2840	0.5950	0.8889	0.9796	0

The dimensionless Power Loss (Rate of working against viscous forces) is given by (34).

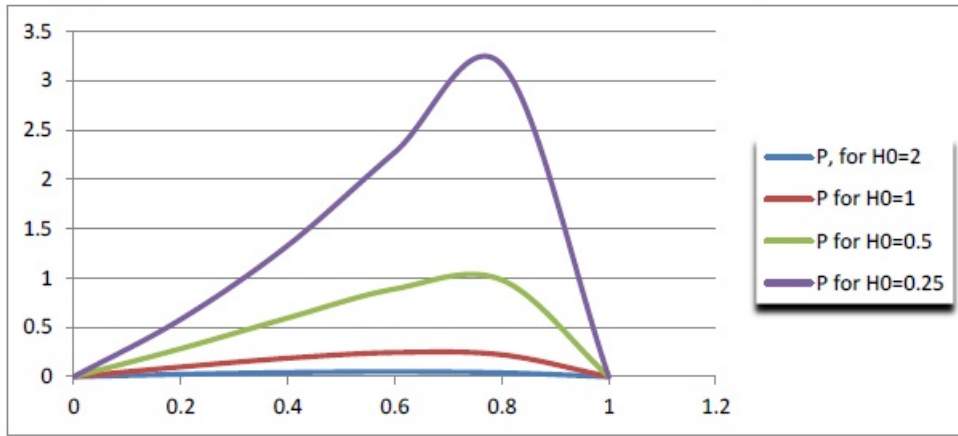
Table 2 : Adiabatic temperature rise versus film thickness ratio

H_0	0	0.5	1.0	1.5	2.0
$\frac{H_p}{Q}$	∞	1.8592655396	0.5794415417	0.2897613307	0.1757751802

Table 3 : Dimensionless power loss versus film thickness ratio

H_0	0	0.5	1.0	1.5	2.0
H_p	∞	1.3944491547	0.7725887222	0.5433024951	0.4218604324

The graph of P versus X for various values of H_0 is as shown below;

**Figure 3: Graph of dimensionless Pressure, P versus dimensionless Cartesian coordinate X**

From figure 1, it is clear that Pressure distribution increases with decreasing H_0 . Since $H_0 = h_0/s_h$, if the shoulder height s_h is kept constant, the graph above indicates that as the outlet film thickness h_0 becomes smaller, the pressure profile increases without any limits. The figure also shows that for large H_0 , there is little pressure build up for a fixed incline slider bearing. From equation (32), As $H_0 \rightarrow 0$, the location of the maximum pressure $X_m \rightarrow 1$. But as $H_0 \rightarrow \infty$, $X_m \rightarrow 1/2$. Further, $H_0 \rightarrow 0$ implies that either $h_0 \rightarrow 0$ or $s_h \rightarrow \infty$. But $H_0 \rightarrow \infty$, implies that either $h_0 \rightarrow \infty$ or $s_h \rightarrow 0$. The situation of $s_h \rightarrow 0$, implies parallel surfaces, and parallel surfaces do not develop pressure. From equation (33), it is observed that $s_h \rightarrow 0$, which corresponds to a parallel film, and $s_h \rightarrow \infty$ both produce $p_m \rightarrow 0$. The shoulder height that produces maximum pressure can be obtained from $\partial p_m / \partial s_h = 0$. Evaluating this gives;

$$(s_h)_{\text{opt}} = \sqrt{2}h_0 \quad (37)$$

Equation (37) will be useful in the design of fixed incline slider bearings. For instance, if the shoulder height s_h is known, one can predict what the minimum outlet film thickness h_0 should be. The shoulder height can then be established by using the safety factor.

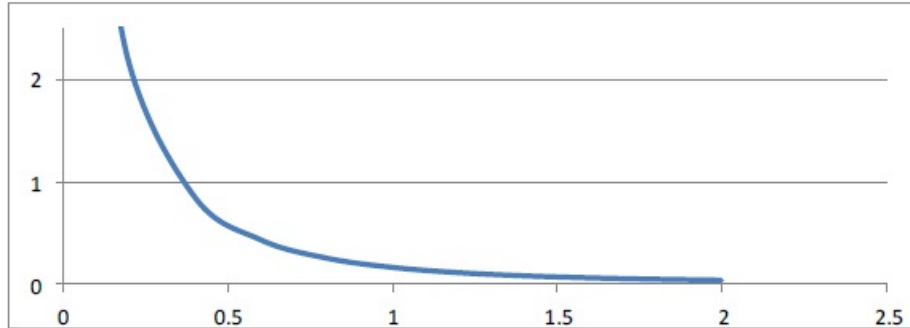


Figure 4: Variation of film thickness ratio with normal load carrying capacity

Figure 2 shows that as $H_0 \rightarrow 0$, the potential of this bearing to support a load increases exponentially. The graph of adiabatic temperature rise versus film thickness ratio is as shown in Figure 3 below;

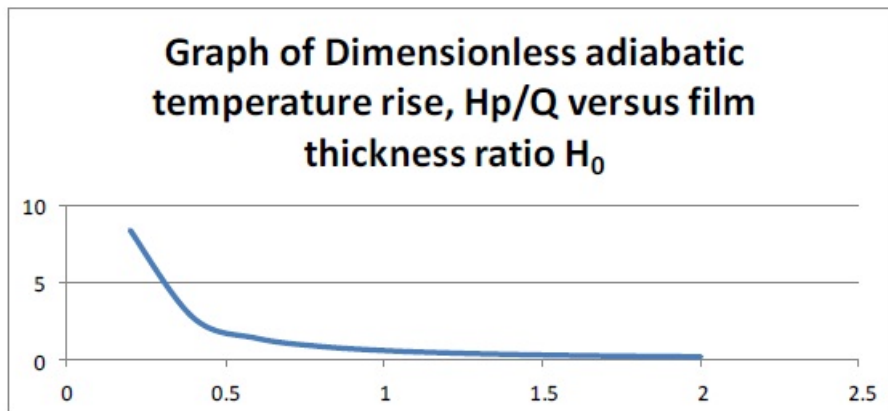


Figure 5: Effect of film thickness ratio on adiabatic temperature rise

A graph of Dimensionless power loss versus film thickness ratio is shown in Figure 4 below;

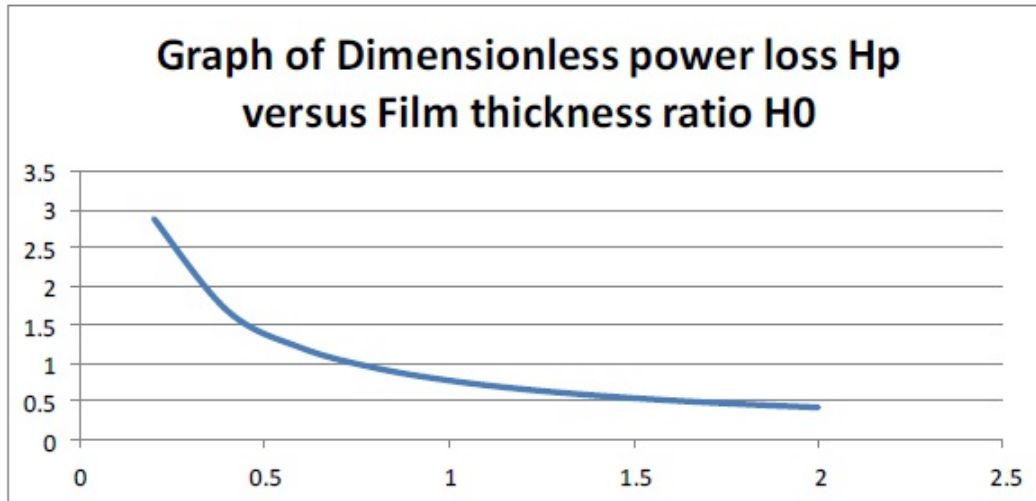


Figure 6: Effect of film thickness ratio on power loss

6. Conclusion

The analysis of the axial variation of various parameters on the flow of the lubricants under hydrodynamic lubrication condition between the plates of a fixed incline slider bearing has been done. The equations governing hydrodynamic flow considered in our study are; the continuity equation, the Navier-stokes equations, the Reynolds equation. The Navier-stokes equation together with the continuity equation is used to derive the Reynolds equation. The Reynolds equation is then used to determine the pressure distribution of the lubricant in a fixed incline slider bearing. The power loss and temperature variation are determined and their variation along the bearing analyzed, discussed and represented graphically. In particular:

1. The pressure profiles are in good agreement with published results of Reynolds equation for the bearing done in two dimensions
2. The temperature profiles are also in good agreement with published results for studies of the thermo-hydrodynamic lubrication analysis of a tilting pad step bearings.]]

Nomenclature

Symbol	Meaning with units if any
--------	---------------------------

A, B, C, D	integration constants
X, Y and Z	Dimensionless length parameters
h	oil film thickness, m
h_m	maximum film thickness, m
h_0	Characteristic length in the z or x directions, m
p	pressure, pa
P	dimensionless pressure
p_0	Characteristic pressure, pa
\mathbf{q}	Fluid velocity, m/s
x, y, z	Velocity components in x -, y - and z - directions respectively, m/s
u_0	Characteristic velocity in the x - direction, m/s
v_0	Characteristic velocity in the y - direction, m/s
z_0	Characteristic velocity in the z - direction, m/s
t	Time, s
T	Characteristic time
τ	Viscous shear stress, N/m^2
ρ	Fluid density, kg/m^3
ρ_m	Maximum fluid density, kg/m^3
η	Absolute viscosity, pas
η_0	Characteristic viscosity, pas
T_0	Characteristic temperature, K
C_p	Specific heat, $Jkg^{-1}K^{-1}$
κ	Thermal conductivity, $Wm^{-1}K^{-1}$
H_0	Oil film thickness in the leading edge, m
∇	Gradient operator
∇^2	Laplacian operator

References

- [1] Vohr J. H., Prediction of operating temperatures of thrust bearings. Journal of Lubrication Technology, 103(1) (1981), 97-106.

- [2] Abdel Latif L. A., Bakr E. M. and Ghobrial M. I., Centrifugal effects of thermo hydrodynamic performance of circular pad thrust bearings, *Journal of Tribology*, 111(3) (2009), 510-517.
- [3] Hashimoto H., Performance characteristics of sector-shaped pad thrust bearings in turbulent inertial flow regime under three types of lubrication conditions. *Journal of Tribology*, 112(3) (1990), 477-484.
- [4] Fenner R. T. and Ali Elsiaie Y. M. H., Three dimensional elasto-hydrodynamic analysis of pivoted pad thrust bearings. *Journal of Mechanical Engineering Science*, 202(1) (1987), 51-62.
- [5] Kiogora P. R., Kinyanjui M. N., Theuri David M., Conservative scheme model of an inclined thrust pad bearing. *International Journal of Engineering Science and Innovative Technology*, 3(1) (2014), 446-453.
- [6] Banwait S. S. and Kadam K. R., The influence of modified viscosity-temperature equation on thermo-hydrodynamic analysis of plain journal bearing, *American Journal of Mechanical Engineering*, 2(6) (2014), 169-177.
- [7] Charitupoulous A., Fouflias D., Papadopoulos C. I., Kaiktsis L. and Fillon M., Computational investigation of thermo-elasto-hydrodynamic (TEHD) lubrication in a textured sector-pad thrust bearing, *Mechanics and Industry*, 15 (2013), 403-411.
- [8] Manyonge A. W., *Elementary Fluid Mechanics, A First Course*, Lambert Academic Publishing, Saarbrücken, Germany, (2013).
- [9] Sahu M., Giri A. K., and Das A., Thermo-Hydrodynamic analysis of a journal bearing using CDF as a tool, *International Journal of Scientific and Research Publications*, 2(9) (2012), 1-7.